Determining the Structure of Silica-Supported Monomeric Vanadium Oxide Catalysts Based on Synthesis Method and Spectral Data from Theoretical Calculations

Joost N. J. van Lingen,*,†,‡ Onno L. J. Gijzeman,† Remco W. A. Havenith,† and Joop H. van Lenthe†

Theoretical Chemistry Group and Group of Inorganic Chemistry and Catalysis, Utrecht University, P.O. Box 80083, 3508 TB Utrecht, The Netherlands

Received: August 23, 2006; In Final Form: February 8, 2007

Infrared and Raman spectra have been calculated for several molecular cluster models for the silica-supported monomeric vanadium oxide catalysts that are proposed in the literature: the pyramid model, the umbrella model, and a model containing two bonds to the support, a V═O group and an OH group. A related model with one bond to the support, a V═O and two OH groups, will also be discussed. From the comparison with literature, it is concluded that two models, the umbrella model and the model with two bonds to the support, are realistic descriptions of actual systems. The presence of a particular compound depends on the method of preparation. The internal V−O distances by themselves are not enough to distinguish between the presented models.

Introduction

Supported vanadium oxide catalysts represent an important class of heterogeneous catalysts that are widely used in chemical industries in various selective oxidation reactions as well as for the selective reduction of NO_x emissions.[1−4] They consist of an active vanadium oxide phase deposited on the surface of a high-surface oxide support, such as SiO_2, Al_2O_3, TiO_2, and ZrO_2. The molecular structure of these supported vanadium oxide species has been studied by a wide variety of spectroscopic techniques, including Raman, ^{51}V NMR, UV−vis- near-infrared, extended X-ray absorption fine structure (EXAFS), X-ray absorption near-edge spectroscopy, electron spin resonance, and X-ray photoelectron spectroscopy.[5−18] Several review papers, which describe the current understanding of these catalytic systems,[18−21] can be found in the literature.

For a low-loaded silica-supported catalyst, which is the focus of this paper, it has been shown that on the surface only monomeric species are present.[6,22−24] There is, however, no definite model that can unambiguously explain all the experimental data collected over the years, although a predominant tendency for the pyramid model[25−31] exists (Figure 1A). Magg et all.[32] have recently discussed the assignment of spectral bands in their paper based on this pyramidal model. They presented spectra for alumina- and silica-supported vanadium oxide but were not able to draw any conclusions for the silica, although they expected that the same vibrations should be present on silica as on alumina. However, we think that the explanation of the spectra should be sought in a different model or perhaps in the presence of multiple molecular structures as discussed in earlier papers.[23,33,34] There are a number of routes to synthesize the vanadium oxide catalyst, each leading to (perhaps not surprisingly) a different structure of the active species.

The most common way of synthesis for the vanadium oxide catalyst is to create first a support and then deposit the VO_x species on top by incipient wetness impregnation techniques.[35] Another interesting method recently described is the co-condensation of monomeric vanadium $VO_2(OH)_2^-$ and Si-$(OC_2H_5)_4$ species in a solution, as described by Nguyen[36] and used before by other groups in a slightly different manner[37−39] Apart from these wet techniques, there is a nonchemical preparation of the supported VO_x species that is used by Freund

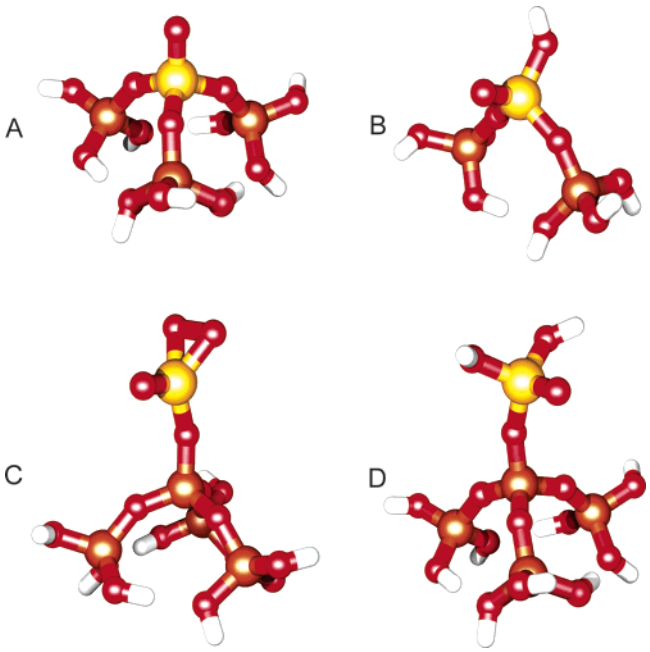

Figure 1. The molecular structure of the six cluster models studied in this paper: (a) the pyramid model consisting of a V═O unit bonded to the support with three Si−O_s−V bonds; (b) a species with two Si−O_s−V support bonds, a V═O, and a V−OH group; (c) the umbrella model with only one support Si−O_s−V bond, a V═O group, and a perturbed oxygen molecule bound to the V-atom; and (d) the hydrogenated version of the umbrella model in which the oxygen molecule is replaced by two OH groups.

* To whom correspondence should be addressed. E-mail address: j.n.j.vanlingen@chem.uu.nl.
† Theoretical Chemistry Group.
‡ Group of Inorganic Chemistry and Catalysis.

10.1021/jp065447u CCC: $37.00
Published on Web 04/25/2007

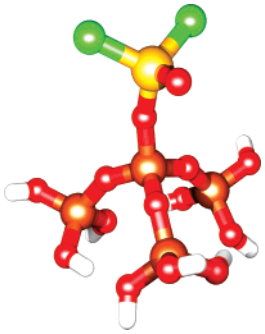

Figure 2. The optimized O_s-VOCl_2 model of Scott et al.[50,56,57]

et al.[32,40−43] They deposit atomic vanadium on an oxide film under ultrahigh vacuum (UHV) by means of an electron-beam evaporator.

With these preparation approaches in mind, we looked at the models presented in the last three decades for the molecular structures of the active VO_x species on top of the supporting material. There is a consensus that the monomeric structure present at low loadings is a distorted tetrahedral around the central vanadium atom and that there are one or more V═O bonds present.[29,44−47] For the incipient wetness technique, it has been concluded from EXAFS experiments[23,48] that the V- atom is surrounded by three O-atoms at 1.78 Å and one O-atom at 1.58 Å. This is as far as the consensus goes. The main difference between the models is the way the tetrahedral VO_4 species is attached to the surface. The pyramid model, introduced in the 1980s (Figure 1A), with three $Si-O_s-V$ bonds connecting it to the surface of the support and a V═O on top is the most popular one.[25−31] Another structure, which has two $Si-O_s-V$ bonds and two V═O bonds, has been presented by Kozlowski et al.[45] This structure has already been discarded as a candidate structure by Bond et al.[49] and later by EXAFS experiments.[23,48] The hydrogenated variant of this structure (Figure 1B) in which one of the V═O bonds is replaced by a V−OH has also been presented in literature.[49−53] In 2004, we introduced the umbrella model[23,33,34] (Figure 1C) in which the vanadium atom is linked to the surface via only one $Si-O_s-V$ bond and further consists of a V═O and a perturbed O_2 molecule linked to the central vanadium atom. We have shown that the model complies with isotope labeling experiments,[33] and it is in agreement with the recent Raman experiments of Keller et al.[54] The oxygen molecule is attached to the vanadium atom with an energy of 352 kJ/mol,[34] which means it will desorb around 1100 K. Thus at 700 K, the highest temperature used by Keller et al.,[54] the umbrella model will be stable. A variation on the umbrella model is obtained when the perturbed O_2 is replaced by two OH groups.[55] This gives a $O═V-(OH)_2$ structure (Figure 1D) with still one bond to the support. Keller et al.[24] have also proposed this structure. A related structure emerged with Cl atoms in place of the OH moieties in the experiments of Scott et al.[50,56,57] (Figure 2).

Theoretical IR and Raman spectra have been calculated with density functional theory (DFT) for all the models described above supported on silica. We compare these theoretical spectra with experimental data found in the literature.[34,36,57]

Experimental Methods

The theoretical spectra were calculated with the GAMESS-UK package.[58] All cluster models were optimized to a maximum gradient of 4.4 10^{-5} using the B3LYP density functional[59,60] and the TZVP basis set.[61] After optimizing, harmonic vibrational frequencies and IR intensities were calculated via an analytical Hessian calculation using the same basis. Only the terminating H-atoms, used to saturate the dangling bonds on the outside of the cluster models, were frozen to prevent them having a large influence on the calculated intensities. This will perhaps influence the low-lying vibrations but will have no influence on the isolated vibrations in the higher-frequency regions.

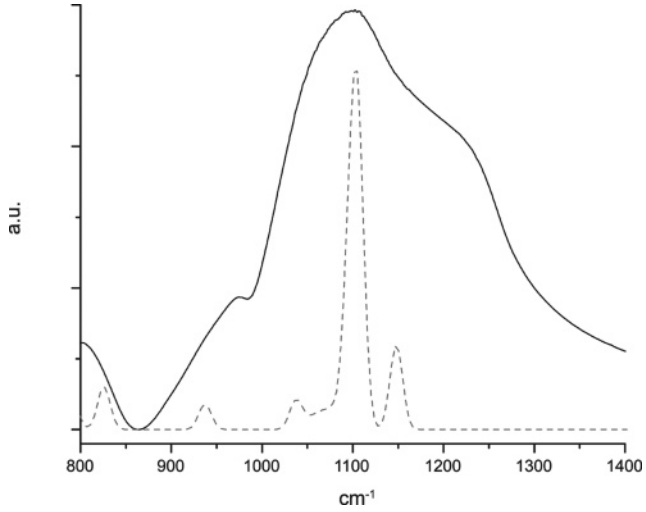

Figure 3. The experimental IR spectrum of silica (solid line) and a theoretical IR spectrum for silica (dotted line). The latter was calculated on the support of model C with the VO_3 group on top replaced with a H-atom.

To test this approach, we have calculated the infrared spectrum for the support of model C (Figure 1C) by replacing the VO_3 unit with one H-atom. A comparison between the theoretical spectrum and an experimental spectrum is shown in Figure 3. The theoretical spectrum (and all others in this paper) has been drawn by giving each vibration the same (10 cm^{-1}) half width. The area underneath the peaks is thus proportional to the calculated intensity of the peak. A scaling factor of 0.98 was needed to shift the largest theoretical peak to this experimental position at 1100 cm^{-1}. Calculations and comparison with experimental values[62] on structures $VOBr_3$, $VOCl_3$, and VOF_3 lead to scaling factors that are respectively 0.93, 0.94, and 0.93. This is in good agreement with the well-known fact that the calculated frequencies calculated at the DFT level of theory are slightly too high, compared with experiments.[63] Commonly an averaged scaling factor of 0.95 is used to correct for this deficiency.[64,65] This factor has been incorporated in all results. However, this is an average. A difference of 1 or 2% leads in this range of frequencies to a difference of 10−20 cm^{-1} that we consider in this paper as normal deficiency by comparing experimental and theoretical results.

The accompanying Raman intensities were calculated in the following manner. As GAMESS-UK does not currently support the calculation of Raman intensities with DFT, the intensities were calculated at the Hartree−Fock (HF) level. The unscaled frequencies differ for HF and DFT so connecting the vibrations was necessary. This was done by visualization of the vibrations in Molden[66] with the constraints that the calculated HF (scaling factor used for HF was 0.85) and DFT frequencies were within 30 cm^{-1} and the corresponding IR intensities were within 20% of each other. The HF Raman intensity was then assigned to the linked DFT frequency of the vibration.

Results

The optimized cluster structures are shown in Figure 1. For these clusters, the distances from the central V-atom to the

TABLE 1: V−O Distances Found after Optimization of the Cluster Models in Figure 1 (Distances Are Represented in Å)

type of distance	pyramid (A)	$(O_s)_2$−VOOH (B)	umbrella (C)	O_s−$VO(OH)_2$ (D)	O_s−$VOCl_2$ (E)
V═O	1.578	1.581	1.580	1.577	1.568
V−O		1.778	1.799/1.799	1.780	2.170/2.169 (Cl)
V−O_s	1.773 (3x)	1.790/1.757	1.778	1.780/1.780	1.747

TABLE 2: Calculated Frequencies and Intensities in IR and Raman for the Active Species on Top of the Support[a]

pyramid				905		1004	1024	1036	1045			
model A				Asym $(Si−O_s)_3−V$		Sym $(Si−O_s)_3−V$	Asym $(O_s)_3−V═O$	V═O	Sym $(O_s)_3−V═O$			
IR				1782		45	903	159	72			
Raman				14.8		0.6	6.3	2.2	23. 6			
O_{s2}−V═O(OH)		632	746	905		1000		1042		3658		
model B		O−H bend	V−OH stretch	Asym $(Si−O_s)_2−V$		Sym $(Si−O_s)_2−V$		V═O		O−H		
IR		265	219	976		700		289		226		
Raman		3.8	2.3	8.4		4.7		19.0		103		
umbrella				903	978			1037				
model C				O−O	Si−O_s−V			V═O				
IR				324	1823			116				
Raman				31.7	6.9			14.2				
O_s−V═$O(OH)_2$	613	635	714	758		986			1049	3664	3368	
model D	Asym $(O−H)_2$ bend	Sym $(O−H)_2$ bend	Sym $V−(OH)_2$ bend	Asym $V−(OH)_2$ bend		Si−O−V		V═O		Asym $(O−H)_2$ stretch	Sym $(O−H)_2$ stretch	
IR	208	281	217	175		1810		101		265	137	
Raman	0.0	1.2	7.8	0.7		11.0		17.01		65.4	115.5	
O_s−V═OCl_2					965			1046				
model E					Si−O_s−V			V═O				
IR					2066			61				

[a] Per cluster, the rows denote frequency, type of vibration, IR intensity (km/mol), and Raman intensity (au) going from top to bottom. The columns have been aligned in such a way that the frequencies (cm^{-1}) of the various clusters are approximately equal. Note that vibrational modes may differ from cluster to cluster.

surrounding O-atoms are tabulated in Table 1. The calculated vibrations, which include the active species on top of the silica support and their corresponding intensities in IR and Raman, are shown in Table 2. Figure 4 shows the resulting theoretical spectra in Raman and IR, respectively, in the range from 800 to 1100 cm^{-1}.

Cluster A (Figure 1A), which is the pyramid model,[25−31] clearly has two distinguishable peaks in the IR. One for the asymmetric $(Si−O_s)_3−V$ vibration at 905 cm^{-1} and one asymmetric $(O_s)_3−V═O$ at 1024 cm^{-1}. In Raman, the band at 905 cm^{-1} stays visible and another peak (symmetric $(O_s)_3−V═O$) at 1045 cm^{-1} becomes dominant. So the most interesting feature here is that the peaks seen in the 1020−1050 cm^{-1} region are highly influenced by the pyramid of O_s atoms underneath it. The pure V═O mode lies inbetween those peaks but has a much lower intensity in both IR and Raman. The symmetric $(Si−O_s)_3−V$ vibration at 1004 cm^{-1} has a very low relative intensity in both IR and Raman and will not be visible in experimental spectra.

Cluster B[49−53] (Figure 1B) with two legs to the support, a V═O group, and an OH group has three peaks in both the IR and Raman spectra between 800 and 1150 cm^{-1}. The first two bands at 905 and 1000 cm^{-1} are related to Si−O_s−V bonds and are more intense in IR than the V═O stretch vibration at 1042 cm^{-1}, which is the most intense in Raman. The OH group gives rise to an O−H stretch vibration at 3658 cm^{-1} and a bend vibration at 630 cm^{-1}. The V−OH stretch at which the hydroxyl group vibrates as a unit lies at 746 cm^{-1}.

The umbrella model (Figure 1C) has, as discussed before,[33,34] an O−O stretch vibration in the perturbed O_2 molecule at 903 cm^{-1}, a Si−O_s−V vibration at 978 cm^{-1}, and a V═O stretch vibration at 1037 cm^{-1}. The middle one is the most intense in IR. The first and last are prominent in Raman.

In the hydrogenated version of the umbrella model[55] (Figure 1D), four vibrations related to the two OH groups, asymmetric bending 613 cm^{-1}, symmetric bending 635 cm^{-1}, asymmetric stretching at 3664 cm^{-1}, and symmetric stretching at 3668 cm^{-1}, are present. When the hydroxyl groups vibrate as a whole it results in a symmetric and an antisymmetric stretching vibration at 714 and 758 cm^{-1}, respectively. In the region of 800−1150 cm^{-1}, the V═O at 1049 cm^{-1} and the Si−O_s−V at 986 cm^{-1} are present, although the former is very weak in the IR spectrum.

For the structure presented by Scott et al.[50,56,57] (Figure 2), the resulting frequencies are presented in Table 3.

Discussion

V−O Distances. From the V−O distances as presented in Table 1, no real distinction can be made between all the cluster models. In all clusters, the V═O distances are 1.58 Å. The remaining V−O distances are always 1.78 Å. It does not matter whether those O-atoms belong to the support, the perturbed oxygen molecule in the umbrella model, or the OH groups in clusters B and D. To distinguish between the models is thus impossible with EXAFS.

Synthesis, Spectra and Structure. *Incipient Wetness Impregnation*. This is the most common way of synthesis in which the VO_x species is deposited on an already-prepared oxidic support.[35] With this technique, the X−O_s−V bonds will be formed by the elimination of H_2O from one V−OH and one

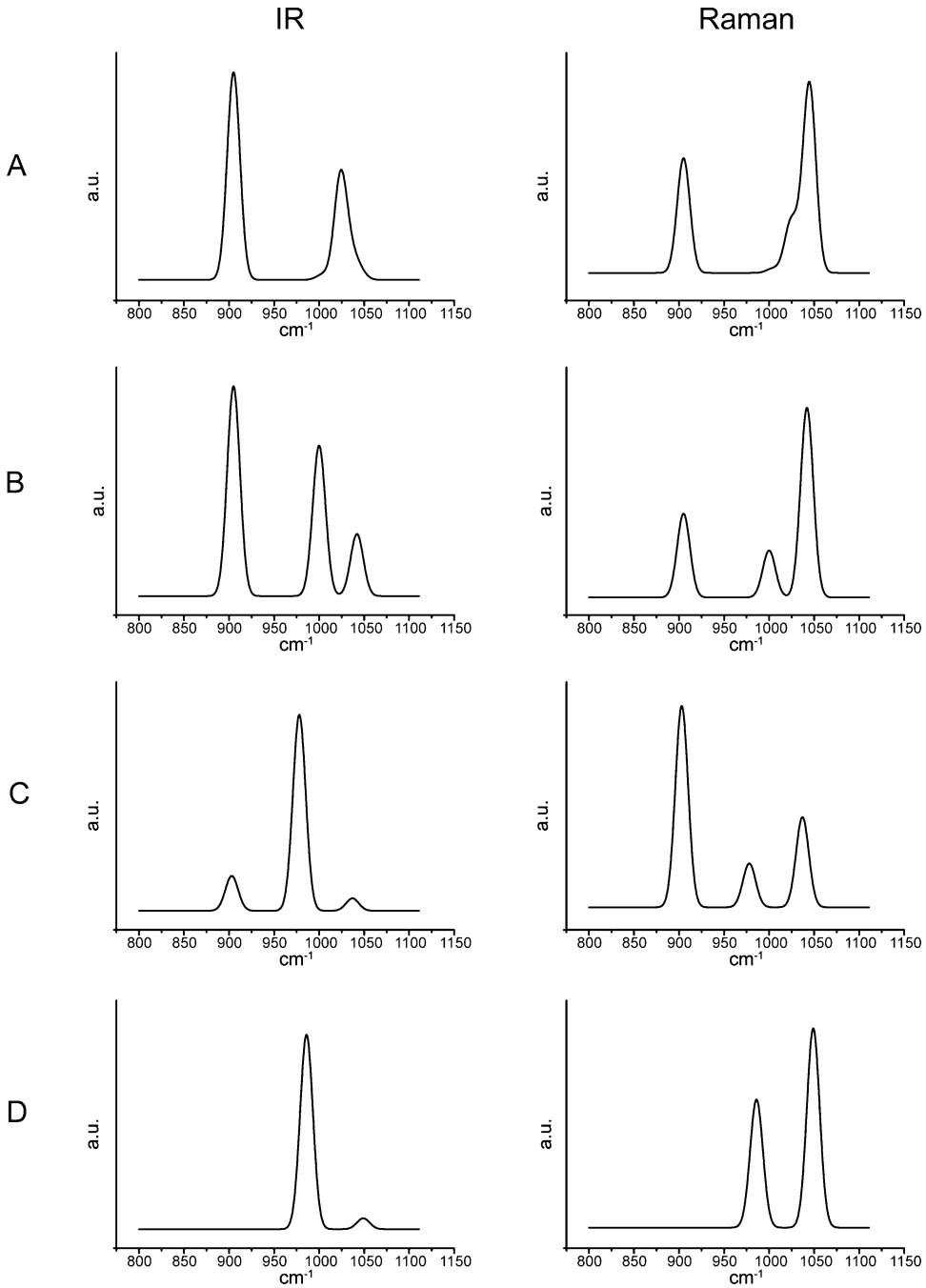

Figure 4. Theoretical IR and Raman spectra in the range of 800−1100 cm^{-1} calculated for the clusters shown in Figure 1. The letters a−e correspond to the letters next to the models in Figure 1.

TABLE 3: IR Frequencies and Intensities Calculated for the $O_sVO(Cl)_2$ Structure Introduced by Scott et al.[50,56,57]

$O_s-V=OCl_2$	frequencies (cm^{-1})	intensities (km/mol)
symmetric $V-Cl_2$	425	124
asymmetric $V-Cl_2$	474	141
$Si-O_s-V$	965	2066
V=O	1046	61

X−OH group. Thus, the number and geometry of available hydroxyl groups at the surface determines the number of $X-O_s-V$ bonds. A model with only one surface bond (Figure 1C−E) can be formed wherever a surface hydroxyl group is available. For the model (Figure 1B) with two surface bonds, a distance of about 3 Å between the hydroxyl groups is required for the formation of the $Si-O_s-V-O_s-Si$ unit. For a pyramid model (Figure 1A), the hydroxyl groups even have to form a triangle with a side of maximum 3 Å on the surface to form the cluster. Zhuravlev[67] and Groppo[68] show in their articles that hydroxyl groups are rather scarce on the silica surface, and the pictures of a hydrated silica surface drawn by Groppo[68] also show that triangles of hydroxyl groups within a feasible distance of each other are almost nonexisting. This means that this method of synthesis has a large chance to generate an active species with only one bond to the surface. This has already been shown experimentally by Scott et al.[50,56,57] When they deposit $OVCl_3$ on top of a Si−OH group in a silica support, only one HCl molecule per adsorbed species is released, which proves that an O_s-VOCl_2 structure (Figure 2) is formed.

Unfortunately, IR spectra of silica are dominated by intense lattice vibrations at 1050 cm^{-1}. Thus, the relevant region of 900−1100 cm^{-1} is difficult to study experimentally for bulk samples. The optimal path length through the silica has to be very small as in the case of the experiments conducted by Scott

et al.[56,57] They show in their IR spectrum[56] peaks at 959 and 1043 cm^{-1}, which were assigned to the $Si-O_s-V$ and a V═O, respectively. The calculated spectrum for this O_s-VOCl_2 model (Figure 2 and Table 3) shows a $Si-O_s-V$ vibration at 965 cm^{-1} and the V═O at 1046 cm^{-1}, which agrees with the assignment of Scott et al. This confirms their proposed structure and indicates once again that our calculations are reasonably accurate.

Compared to the paucity of IR data, an abundance of Raman spectra are available in this region; however, most of them concern high-loaded catalysts, which are not the focus of this paper. In our previous paper,[34] we concluded that three peaks for the VO_4 species are present in the Raman spectra for the low-loaded catalyst: one clear sharp peak at 1040 cm^{-1} and a weak very broad band around 918 cm^{-1}. The peak at 980 cm^{-1} shows an increase in intensity with increasing loading in the region of 0−4 V. Therefore, it cannot be completely attributed to the silica support. Thus, these three peaks should be reproduced by our models.

The pyramid model (Figure 1A) does not have a peak at around 980 cm^{-1} in contrast to our experimental observations.[34] The symmetric $(Si-O_s)_3-V$ vibration at 1004 cm^{-1} has a too low intensity in Raman. The asymmetric $(O_s)_3-V═O$ band at 1024 cm^{-1} has a Raman intensity that might make it visible as a shoulder on its symmetric counterpart as shown in Figure 4A. To assign this vibration to the band seen at 980 cm^{-1}, it has to shift downward for 40 cm^{-1}. After applying the usual correction factor of 0.95, the V═O stretch vibration is calculated almost at the right frequency, and it is expected that all three V−O stretch-dominated vibrations would shift in the same direction. Therefore, it is highly unlikely that the band seen at 980 cm^{-1} should be assigned to the asymmetric $(O_s)_3-V═O$ vibration calculated at 1024 cm^{-1}. The missing peak, the evidence already presented in our previous paper,[34] and the way of synthesis discard the pyramid model as a suitable model for the result of incipient wetness impregnation.

In the theoretical spectrum of the hydrogenated umbrella model (Figure 1D), the peak around 918 cm^{-1} is missing, which is caused by the replacement of the perturbed O_2 molecule by two OH groups. Thus, this model is not able to explain the experimental observations.[34]

This leaves two models to explain the observed spectrum (i.e., the model with two support bonds (Figure 1B) and the umbrella model (Figure 1C)) as they have three peaks visible in roughly the right spectral area. The largest distinction between them is the presence of the OH group in cluster B, which would give rise to a O−H stretch vibration at 3658 cm^{-1}. In the experimental data,[34] there was no peak present that could point to an OH group. This favors the umbrella model as the one produced by incipient wetness impregnation.

Co-Condensation. The co-condensation of monomeric vanadium $VO_2(OH)_2^-$ and $Si(OC_2H_5)_4$ at a pH inbetween 5 and 6 in a solution containing template was described by Nguyen et al.[36] With this technique, the support is generated at the same time as the $VO_2(OH)_2^-$ is deposited. This increases the chance that multiple bonds to the silica precursor are formed from the VO_4 species. Nguyen et al. report in their paper[36] that they suspect that two species are present on the surface: the pyramid model (Figure 1A) and the two-legged variant with one OH group on top (Figure 1B). In their Raman spectrum,[36] an intense band is found at 1037 cm^{-1}, which is the V═O stretch vibration. Next to this vibration, a very broad band at 920 cm^{-1} is visible. There is also a peak present at 980 cm^{-1} that they attribute to the elongation of the Si−OH groups of the silica support. Comparing these observed frequencies with Table 2 leads to almost the same reasoning as before in the discussion of the incipient wetness impregnation technique. When we look at the spectral region of 800−1200 cm^{-1}, both the umbrella structure (Figure 1C) and model B (Figure 1B) are possibly formed on the surface. In contrast to our Raman observations,[34] Nguyen et al.[36] do also observe an OH vibration at 3658 cm^{-1}. This is indeed the frequency we calculated for the OH stretch vibration in model B. So the co-condensation preparation method does at least lead to one distinct model on the surface, model B. However is cannot be excluded that the umbrella model (model C) is present also.

Vacuum Deposition. In the preparation of the supported VO_x species, which is used by Freund et al.,[32,40−43] first an oxide film is created under UHV. Then atomic vanadium is deposited in an oxygen ambient atmosphere of 1×10^{-7} mbar by means of an electron-beam evaporator. It is not clear to us what kind of structure for VO_x is to be expected. It will depend on how much O_2 the atomic vanadium picks up before it lands on the surface. Freund et al. conclude that a low temperature (60K) is needed to avoid agglomeration.[42] In their STM measurements, it is seen that via diffusion polymeric species are formed at higher temperatures. From this we conclude that the bonds formed with the oxidic surface of the support are weak.

Their IR spectrum for a monolayer coverage only reveals one peak at 1046 cm^{-1}, which is assigned to the V═O vibration.[32] For lower vanadium coverage, there is also a band visible at 1005 cm^{-1} shifting to 1035 cm^{-1} and attributed to $Si-O_s$ vibrations. When these IR results are compared with Table 2, it is impossible to find a model that fits this spectrum, which is consistent with the findings of Freund et al.[32] for their silica-supported spectra. The pyramid model should have a very intense IR band at 905 cm^{-1}. The same applies to the model with two bonds to the support (Figure 1B). The models with only one bond to the surface have the $Si-O_s-V$ vibration at 978 cm^{-1}, which should be very intense in IR. Next to this, no OH groups are present, as one would expected with this method of synthesis and as Freund et al. mention in their paper.[69] This discards models B and D in Figure 1.

The Structure and Water. In the previous sections, only the dehydrated condition for the molecular structure of silica-supported vanadium oxide catalysts is considered. This makes the spectral region of 800−1200 cm^{-1} the most interesting. V−OH groups, however, are present in structures B and D (Figure 1B,D) and have vibrations around 3660 and 3360 cm^{-1}, respectively, as can be seen from Table 3. For the synthesis method used by Nguyen et al.[36] the presence of the OH groups is a logical consequence of the method, and they do indeed observe an OH vibration at 3658 cm^{-1}. Keller et al.[24] also proposed this structure (D) as being created by the rehydration of the pyramid model. When they cool their dehydrated samples to 77 K, an additional sharp band at 3660 cm^{-1} is seen and the V═O vibration shifts from 1046 to 1035 cm^{-1}. They attribute this effect to the addition of two molecules of water to a pyramid structure with the concomitant formation of two Si−OH groups. This involves breaking bonds at 77 K. It is much more likely that at low temperatures a water molecule physisorbs onto the umbrella structure. This will affect the V═O frequency, the O−O frequency, and will result in the appearance of OH vibrations. Calculated Raman spectra for the resulting hydrated species are shown in Figure 5. Compared to the dehydrated spectrum, the peak at 915 cm^{-1} shifts to a higher wavenumber (930 cm^{-1}) while the V═O shifts to a lower wavenumber. In the 3000−4000 cm^{-1} range, a peak at 3660 cm^{-1} appears. These

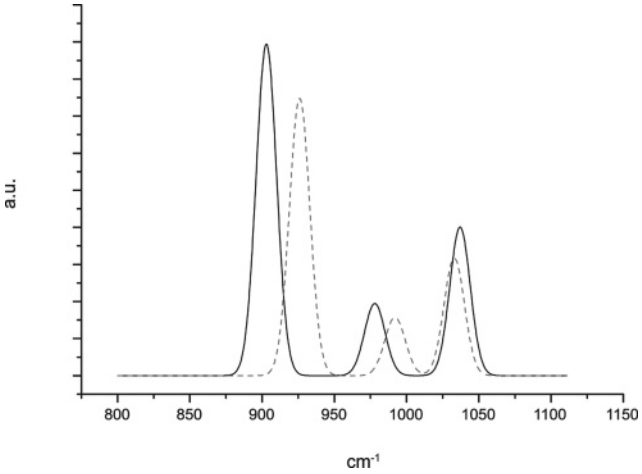

Figure 5. Calculated Raman spectra the umbrella model (Figure 1C) with (dashed line) or without physisorbed water (solid line).

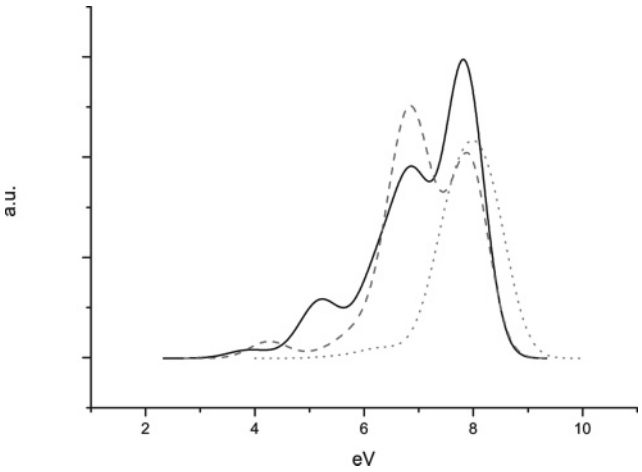

Figure 6. Calculated UV−vis spectra for the umbrella model with physisorbed water (dashed line), the umbrella model without physisorbed water (solid line), and the model proposed by Keller et al., Figure 1d (dotted line).

effects are exactly those reported by Keller et al.[24] for low-vanadium loadings.

Van der Voort et al.[70] showed with UV−vis that the catalyst is highly susceptible to water. After a few minutes, even the most perfect white sample turned orange. Their spectra show a large absorption increase in the visible region. Figure 6 shows the same trend for the calculated UV−vis spectra for the umbrella model. The hydrated species shows a clear shift of the absorption to the visible range. The calculated spectrum for model D (Figure 1D), which is reported by Keller et al.[24] to appear by hydration of the catalyst, shows an even higher start of the absorption then the dehydrated umbrella model and so cannot explain the change in color reported by Van der Voort et al. .[70] Thus it appears that only the umbrella model is capable of explaining the spectra in both hydrated and dehydrated (physisorbed water) conditions.

Conclusion

It is not possible to make a distinction between our different models for the VO_4 unit by the use of EXAFS because there are no significant differences between the models regarding the V−O distances. On the basis of experimental and theoretical IR and Raman spectra, it can be concluded that for the incipient wetness impregnation techniques[35] the umbrella model (Figure 1C) poses as a good candidate for the VO_4 species on the surface. The co-condensation technique introduced by Nguyen et al.[36] leads to two structures. Model B (Figure 1B) will always be present; next to this structure the umbrella model (Figure 1C) is present. The evaporation of atomic vanadium under UHV on to a oxidic support used by Freund et al.[32,40−43] gives a structure with a weak V-substrate interaction. It cannot be defined by comparion with the models in this paper. The umbrella model is able to explain both Raman and UV−vis spectral data in both dehydrated and hydrated conditions.

Acknowledgment. We thank Professor B.M. Weckhuysen for stimulating discussions. We acknowledge financial support from NWO/NCF for the use of supercomputer time on TERAS and ASTER, SARA, The Netherlands, Project Number, SGO32.

References and Notes

(1) Gro Nielsen, U.; Topsoe, N.-Y.; Brorson, M.; Skibsted, J.; Jakobsen, H. J. *J. Am. Chem. Soc.* **2004**, *126*, 4926.
(2) Szakacs, S.; Altena, G. J.; Fransen, T.; Van Ommen, J. G.; Ross, J. R. H. *Catal. Today* **1993**, *16*, 237.
(3) Topsoe, N.-Y.; Topsoe, H. *Catal. Today* **1991**, *9*, 77.
(4) Turco, M.; Lisi, L.; Pirone, R.; Ciambelli, P. *Appl. Catal., B* **1994**, *3*, 133.
(5) Brückner, A.; Rybarczyk, P.; Kosslick, H.; Wolf, G.-U.; Baerns, M. *Stud. Surf. Sci. Catal.* **2002**, *142*, 1141.
(6) Burcham, L. J.; Deo, G.; Gao, X.; Wachs, I. E. *Top. Catal.* **2000**, *11/12*, 85.
(7) Das, N.; Eckert, H.; Hu, H.; Wachs, I. E.; Walzer, J. F.; Feher, F. J. *J. Phys. Chem.* **1993**, *97*, 8240.
(8) Deo, G.; Turek, A. M.; Wachs, I. E.; Machej, T.; Haber, J.; Das, N.; Eckert, H.; Hirt, A. M. *Appl. Catal., A* **1992**, *91*, 27.
(9) Haber, J.; Nowak, P.; Serwicka, E. M.; Wachs, I. E. *Bull. Pol. Acad. Sci., Chem.* **2000**, *48*, 337.
(10) Harlin, M. E.; Niemi, V. M.; Krause, A. O. I.; Weckhuysen, B. M. *J. Catal.* **2001**, *203*, 242.
(11) Jhansi Lakshmi, L.; Ju, Z.; Alyea, E. C. *Langmuir* **1999**, *15*, 3521.
(12) Lapina, O. B.; Khabibulin, D. F.; Shubin, A. A.; Bondareva, V. M. *J. Mol. Catal., A* **2000**, *162*, 381.
(13) Olthof, B.; Khodakov, A.; Bell, A. T.; Iglesia, E. *J. Phys. Chem. B* **2000**, *104*, 1516.
(14) Ruitenbeek, M.; van Dillen, A. J.; de Groot, F. M. F.; Wachs, I. E.; Geus, J. W.; Koningsberger, D. C. *Top. Catal.* **2000**, *10*, 241.
(15) Tanaka, T.; Yanmashita, H.; Tsuchitani, R.; Funabiki, T.; Yoshida, S. *J. Chem. Soc., Faraday Trans.* **1988**, *84*, 2987.
(16) Vuurman, M. A.; Wachs, I. E. *J. Mol. Catal.* **1992**, *77*, 29.
(17) Wachs, I. E.; Chen, Y.; Jehng, J.-M.; Briand, L. E.; Tanaka, T. *Catal. Today* **2003**, *78*, 13.
(18) Weckhuysen, B. M.; Keller, D. E. *Catal. Today* **2003**, *78*, 25.
(19) Bond, G. C.; Flamerz-Tahir, S. *Appl. Catal.* **1991**, *71*, 1.
(20) Deo, G.; Wachs, I. E.; Haber, J. *Crit. Rev. Surf. Chem.* **1994**, *4*, 141.
(21) Wachs, I. E.; Weckhuysen, B. M. *Appl. Catal., A* **1997**, *157*, 67.
(22) Gao, X.; Bare, S. R.; Weckhuysen, B. M.; Wachs, I. E. *J. Phys. Chem. B* **1998**, *102*, 10842.
(23) Keller, D. E.; de Groot, F. M. F.; Koningsberger, D. C.; Weckhuysen, B. M. *J. Phys. Chem. B* **2005**, *109*, 10223.
(24) Keller, D. E.; Koningsberger, D. C.; Weckhuysen, B. M. *J. Phys. Chem. B* **2006**, *110*, 14313.
(25) Anpo, M.; Sunamoto, M.; Che, M. *J. Phys. Chem.* **1989**, *4*, 1187.
(26) Bond, G. C.; Könog, P. *J. Catal.* **1982**, *77*, 309.
(27) Deo, G.; Wachs, I. E. *J. Catal.* **1991**, *129*, 307.
(28) Hardcastle, F. D.; Wachs, I. E. *J. Phys. Chem.* **1991**, *95*, 5031.
(29) Le Coustumer, L. R.; Taouk, B.; Le Meur, M.; Payen, E.; Guelton, M.; Grimblot, J. *J. Phys. Chem.* **1988**, *92*, 1230.
(30) Ramis, G.; Cristiani, C.; Forzatti, P.; Busca, G. *J. Catal.* **1990**, *124*, 574.
(31) Went, G. T.; Oyama, S. T.; Bell, A. T. *J. Phys. Chem.* **1990**, *94*, 4240.
(32) Magg, N.; Immaraporn, B.; Giorgi, J. B.; Schroeder, T.; Baumer, M.; Dobler, J.; Wu, Z.; Kondratenko, E.; Cherian, M.; Baerns, M.; Stair, P. C.; Sauer, J.; Freund, H.-J. *J. Catal.* **2004**, *226*, 88.
(33) Gijzeman, O. L. J.; van Lingen, J. N. J.; van Lenthe, J. H.; Tinnemans, S. J.; Keller, D. E.; Weckhuysen, B. M. *Chem. Phys. Lett.* **2004**, *397*, 277.
(34) van Lingen, J. N. J.; Gijzeman, O. L. J.; van Lenthe, J. H.; Weckhuysen, B. M. *J. Catal.* **2006**, *239*, 34.
(35) Weckhuysen, B. M.; de Ridder, L. M.; Schoonheydt, R. A. *J. Phys. Chem.* **1993**, *97*, 4756.
(36) Nguyen, L. D.; Loridant, S.; Launay, H.; Pigamo, A.; Dubois, J. L.; Milet, J. M. M. *J. Catal.* **2006**, *237*, 38.

(37) Ballarini, N.; Cavani, F.; Ferrari, M.; Catani, R.; Cornaro, U. *J. Catal.* **2003**, *213*, 95.
(38) Dutoit, D. C. M.; Reiche, M. A.; Baiker, A. *Appl. Catal., B* **1997**, *13*, 275.
(39) Wang, C.-B.; Deo, G.; Wachs, I. E. *J. Catal.* **1998**, *178*, 640.
(40) Frank, M.; Bäumer, M.; Kühnemuth, R.; Freund, H.-J. *J. Phys. Chem. B* **2001**, *105*, 8569.
(41) Frank, M.; Kühnemuth, R.; Bäumer, M.; Freund, H.-J. *Surf. Sci.* **2000**, *454*−*456*, 968.
(42) Immaraporn, B.; Magg, N.; Kaya, S.; Wang, J.; Bäumer, M.; Freund, H.-J. *Chem. Phys. Lett.* **2004**, *392*, 127.
(43) Magg, N.; Giorgi, J. B.; Frank, M. M.; Immaraporn, B.; Schroeder, T.; Bäumer, M.; Freund, H.-J. *J. Am. Chem. Soc.* **2004**, *126*, 3616.
(44) Eckert, H.; Wachs, I. E. *J. Phys. Chem.* **1989**, *93*, 6796.
(45) Kozlowski, R.; Pettifer, R. F.; Thomas, J. M. *J. Phys. Chem.* **1983**, *87*, 5176.
(46) Miyamoto, A.; Yamazaki, Y.; Inomata, M.; Murakami, Y. *J. Phys. Chem.* **1981**, *85*, 2366.
(47) Wachs, I. E.; Saleh, R. Y.; Chan, S. S.; Cherish, C. C. *Appl. Catal.* **1985**, *15*, 339.
(48) Anpo, M.; Higashimoto, S.; Matsuoka, M.; Zhanpeisov, N.; Shioya, Y.; Dzwigaj, S.; Che, M. *Catal. Today* **2003**, *78*, 211.
(49) Bond, G. C.; Perez Zurita, J.; Flamerz, S.; Gellings, P. J.; Bosch, H.; Van Ommen, J. G.; Kip, B. J. *Appl. Catal.* **1986**, *22*, 361.
(50) Deguns, E. W.; Taha, Z.; Meitzner, G. D.; Scott, S. L. *J. Phys. Chem. B* **2005**, *109*, 5005.
(51) Ferreira, M. L.; Volpe, M. *J. Mol. Catal., A* **2000**, *164*, 281.
(52) Khaliullin, R. Z.; Bell, A. T. *J. Phys. Chem. B* **2002**, *106*, 7832.
(53) Vittadina, A.; Selloni, A. *J. Phys. Chem. B* **2004**, *108*, 7337.
(54) Keller, D. E.; Visser, T.; Soulimani, F.; Koningsberger, D. C.; Weckhuysen, B. M. *Vib. Spectrosc.* **2007**, *43*, 140.
(55) Schoonheydt, P.
(56) Rice, G. L.; Scott, S. L. *J. Mol. Catal., A* **1997**, *125*, 73.
(57) Rice, G. L.; Scott, S. L. *Langmuir* **1997**, *13*, 1545.
(58) Guest, M. F.; Bush, I. J.; van Dam, H. J. J.; Sherwood, P.; Thomas, J. M. H.; van Lenthe, J. H.; Havenith, R. W. A.; Kendrick, J. *Mol. Phys.* **2005**, *103*, 719.
(59) Hertwig, R. H.; Koch, W. *Chem. Phys. Lett.* **1997**, *268*, 345.
(60) Stephens, P. J.; Devlin, F. J.; Chabalowski, C. F.; Frisch, M. J. *J. Phys. Chem.* **1994**, 11623.
(61) Ahlrichs, R.; Taylor, P. R. *J. Chim. Phys. Phys.-Chim. Biol.* **1981**, *78*, 315.
(62) Socolsky, C.; Brandán, S. A.; Altabef, A. B.; Varetti, E. L. *THEOCHEM* **2004**, *672*, 45.
(63) Dmitrenko, O.; Huang, W.; Polonova, T. E.; Francesconi, L. C.; Wingrave, J. A.; Teplyakov, A. V. *J. Phys. Chem. B* **2003**, *107*, 7747.
(64) Scott, A. P.; Radom, L. *J. Phys. Chem.* **1996**, *100*, 16502.
(65) Wong, M. W. *Chem. Phys. Lett.* **1996**, *256*, 391.
(66) Schaftenaar, G.; Noordik, J. H. *J. Comput.-Aided Mol. Des.* **2000**, *14*, 123.
(67) Zhuravlev, T. *Colloids Surf., A* **2000**, *173*, 1.
(68) Groppo, E.; Lamberti, C.; Bordiga, S.; Spoto, G.; Zecchina, A. *Chem. Rev.* **2005**, *105*, 115.
(69) Magg, N.; Giorgi, J. B.; Schroeder, T.; Bäumer, M.; Freund, H.-J. *J. Phys. Chem. B* **2002**, *106*, 8756.
(70) van der Voort, P.; White, M. G.; Mitchell, M. B.; Verberckmoes, A. A.; Vansant, E. F. *Spectrochim. Acta* **1997**, *53*, 2181.